Environmental Advances 8 (2022) 100208

Contents lists available at ScienceDirect

Environmental Advances

journal homepage: www.sciencedirect.com/journal/environmental-advances

Effects of trabectedin in the zebrafish *Danio rerio:* from cells to larvae

Évila Pinheiro Damasceno [a], Ives Charlie-Silva [b], Glaucia Maria Machado-Santelli [b], Anali M. B. Garnique [b], João Agostinho Machado-Neto [b], Simone Aparecida Teixeira [b], Paula C. Jimenez [c], Diana Carneiro [a], Amadeu M.V.M. Soares [a], Leticia V. Costa-Lotufo [b], Susana Loureiro [a], Maria D. Pavlaki [a,*]

[a] *CESAM - Centre for Environmental and Marine Studies, Department of Biology, University of Aveiro, Campus Universitário de Santiago, 3810-193 Aveiro, Portugal*
[b] *Instituto de Ciências Biomédicas, Universidade de São Paulo, 05508-900 São Paulo, SP, Brazil*
[c] *Departamento de Ciências do Mar, Instituto do Mar, Universidade Federal de São Paulo, 11070-100 Santos, SP, Brazil*

ARTICLE INFO

Keywords:
Anticancer agent
Zebrafish locomotor behavior
ZFL cells
Developmental toxicity
Cytotoxicity

ABSTRACT

Anticancer agents pose a great environmental risk due to their high toxicity. The aim of the current study is to assess the toxicity of trabectedin, a cytotoxic but atypical DNA binder, to liver cell line (ZFL) and embryo-larvae of the zebrafish *Danio rerio* employing an innovative approach. In ZFL cells, trabectedin cytotoxicity was measured using MTT and Trypan blue exclusion assay, and cell morphology was evaluated by fluorescence-activated cell sorting (FACS) and by immunofluorescence analysis. Trabectedin was 60-fold more toxic to ZFL cells than to zebrafish embryo-larvae in terms of mortality/cell viability, with mortality being observed in 42.7 $\mu g.L^{-1}$ for embryo-larvae and non-viability in 0.04 $\mu g.L^{-1}$ for cultured cells. Immunofluorescence staining showed morphology alterations of ZFL-cells exposed to trabectedin in a dose-dependent manner, from 0.04 to 0.15 $\mu g.L^{-1}$. Furthermore, trabectedin induced morphological abnormalities to zebrafish embryo-larvae, such as tail malformations, pericardial edema and lack of equilibrium at concentrations lower than 50.3 $\mu g.L^{-1}$. Regarding larvae behavior analysis, trabectedin increased velocity and total distance covered by zebrafish exposed to 42.7 $\mu g.L^{-1}$ under dark conditions. These results reveal trabectedin to be toxic in both *in vitro* and *in vivo* zebrafish models, and thus the occurrence and persistence of this anticancer agent in the environment may represent a potential risk factor to the biota.

1. Introduction

Dozens of millions of patients receive worldwide chemotherapy (Ferlay et al., 2019) and predictions indicate a considerable growth on the number of cancer cases, consequently, leading to the increased use of anticancer agents (AAs) (Didkowska et al., 2016). Following their administration to patients, AAs and respective metabolites thereof are released into the environment as a result of a limited efficacy of waste water treatment plants for both domestic and hospital residual waters (Kovács et al., 2016). Several studies demonstrated the presence of AAs in environmental aquatic systems, such as, cisplatin, etoposide, doxorubicin, cyclophosphamide and tamoxifen at concentrations ranging from 0.22 to 86.2 $ng.L^{-1}$ in river waters, while in groundwater, AAs levels were from 2.1 up to 29.7 $ng.L^{-1}$ in (Kosjek and Heath, 2011; Santana-Viera et al., 2016). Due to their mechanisms of action that most commonly encompass interactions with DNA, AAs are genotoxic, carcinogenic, mutagenic and/or teratogenic and may promote adverse effects in aquatic organisms, mainly under chronic exposures (Parrella et al., 2014a). In this scenario, the academic community warns that the presence of AAs in drinking water has been detected, putting the environment and human health at risk (Santos et al., 2017). Nevertheless, the presence of AAs in aquatic environments and their impact on both aquatic biota and human health have not yet been adequately studied (Kovács et al., 2016).

Among AAs, trabectedin is an antitumor chemotherapy drug initially isolated from the marine ascidian *Ecteinascidia turbinata* and currently obtained semi-synthetically (D'Incalci and Galmarini, 2010) through a bacterial intermediate. Trabectedin is used in the treatment of soft tissue sarcoma, entering the European market in 2007 and, eight years later, the American one (EMA, 2015; Gordon et al., 2016). This molecule upholds its anticancer effects by binding to specific guanine-rich sequences of the DNA minor groove, then affecting repair mechanisms,

* Corresponding author. University of Aveiro, Department of Biology, Campus Universitário de Santiago, 3810-193, Aveiro, Portugal.
E-mail address: maria.pavlaki@ua.pt (M.D. Pavlaki).

https://doi.org/10.1016/j.envadv.2022.100208
Received 3 March 2022; Accepted 3 March 2022
Available online 4 March 2022

transcription regulation and tumor microenvironment (Larsen et al., 2016). Differently from typical DNA-intercalators (e.g. temozolomide and platinum compounds), which are cytotoxic at high concentrations (μg.L^{-1}), trabectedin is active at lower concentrations (ng.L^{-1} to μg.L^{-1}) (D'Incalci et al., 2014). Ongoing studies and clinical trials have further revealed trabectedin as a promising treatment of other types of tumors, as osteosarcoma and colorectal ones (Higuchi et al., 2019; Jimenez et al., 2020; Zhu et al., 2019).

Considering trabectedin's increasing use in treatment schemes, alone and in combination with other AAs in targeted therapies (Gordon et al., 2016), there is a high probability of its presence already occurring in the environment. Therefore, it is crucial to understand the effects of trabectedin in aquatic systems, along with insight on its persistence in the environment (half-life time) and detection values in water, sewage sludge and wastewater treatment effluents (Kümmerer et al. 2016). Most of the available studies address the effects of trabectedin in mammals and non-human test models, focusing on direct human health effects as aim to better understand the antitumor potential of this drug (Higuchi et al., 2019; Zhu et al., 2019). Therefore, there is an important gap on information regarding the environmental hazard of trabectedin.

When it comes to AAs, there is ecotoxicological information in the literature to diverse taxa of aquatic organisms. In bacterial species, 5-fluouracil induced growth inhibition at levels below 0.1 mg.L^{-1}, while the EC_{50}s found after 18h to *Kurthia gibsonii* and *Pseudomonas fluorescens* were 8 μg.L^{-1} and 3 μg.L^{-1}, respectively (Załeska-Radziwiłł et al., 2014). The exposure for 21 days to cisplatin affected the reproduction output of the crustacean *Daphnia magna*, with an EC_{50} value of 16 μg.L^{-1} (Parrella et al., 2014b). Regarding effects to *Danio rerio,* cyclophosphamide caused malformations in embryos when exposed to 68 μg.L^{-1} after 7 days (Li et al., 2022). Gajski et al. (2016) used the zebrafish liver (ZFL) cell line, the human hepatoma (HepG2) cells, and the human peripheral blood lymphocytes (HPBLs) to assess the toxicity of 5-fluouracil, cisplatin and etoposide and showed that the non-target ZFL cells were more sensitive than cancer cells. The increased hazard of AAs to non-target organisms and cells reinforces the need to explore the ecotoxicological potential of trabectedin.

In this context, the present study aims to investigate the effects of exposure to lethal and sublethal concentrations of the AA trabectedin in both *in vivo* and *in vitro* zebrafish. The present study was designed to provide insight into the environmental toxicity of trabectedin, allowing the better understanding of whether the disposal and dispersion of trabectedin in the environments could affect freshwater fish. Besides, this study aimed to establish the feasibility of the *in vitro* cellular model to predict the whole animal effects.

2. Material and methods

2.1. Test chemical and preparations of test solutions

Trabectedin (>99% purity, CAS No. 114899-77-3) was purchased from Biorbyt, Ltd. (Cambridge, UK). Information on the chemical properties of trabectedin can be found in Supporting Information (Table S1). The stock solution was carefully prepared by dissolving trabectedin in dimethyl sulfoxide (DMSO) (99.9% Fisher) at a concentration of 7.62 mg.L^{-1}, as done by Manda et al. (2020) and stored at -80°C for a maximum of 6 months. Aliquots were thawed for each new experiment to avoid degradation, and then diluted with cell culture medium to the desired concentrations.

2.2. Animals and cell cultures

All *in vitro* experiments were performed using the ZFL cell line. ZFL cells derived from normal liver of adult zebrafish were obtained from American Type Culture Collection (ATCC number: CRL-2634) through the *Banco de Células do Rio de Janeiro*, Brazil (BCRJ-0256) (Ghosh et al., 1994). Cells were tested for mycoplasma detection to exclude contamination and authenticated by the supplier. Cells were cultured under a humidified atmosphere at 28°C in a medium composed of 50% Leibovitz L-15, 35% Dulbecco's Modified Eagle Medium (DMEM) high glucose, and 15% Ham F-12, supplemented with 3.6 g.L^{-1} HEPES, 0.15 g.L^{-1} $NaHCO_3$, 99.9 mg.L^{-1} insulin, 33.7 μg.L^{-1} EGF (Epicatechin gallate), 0.1% penicillin/streptomycin and 5% heath inactivated Fetal bovine serum (FBS).

All *in vivo* experiments were performed using embryo-larvae zebrafish (*Danio rerio*). Wild-type AB strain embryos were obtained from a laboratory culture kept at the Department of Biology (University of Aveiro, Portugal), in a zebrafish facility with a provisional operating permit from General Directorate of Food and Veterinary (DGAV) for raising and use of zebrafish. Fish were maintained in controlled conditions; the temperature was kept at 26 ± 1°C and a 16:8 h (light: dark) photoperiod cycle was maintained. The water culture medium composed of carbon filtered water with 0.34 g L^{-1} marine salt was used in the preparation of test solutions of all experiments performed (Almeida et al., 2019).

2.3. Cytotoxicity tests

Two tests were used to investigate toxicity towards ZFL cell line, the 3-(4,5-dimethylthiazol-2-yl)-2,5-diphenyltetrazolium bromide (MTT) reduction assay (Mosmann, 1983) and the Trypan blue (TB) exclusion test (Lachner et al., 2015). Test range concentrations were chosen based on previous data for the toxicity of tumor cells (Abate et al., 2020).

For the MTT assay, ZFL cells were first seeded on 96-well plates with a cell density of 1×10^4 per well (5×10^4 cells/mL) and incubated overnight at 28°C. On the next day, the test compounds were added (trabectedin at 0.024 ng.L^{-1}, 0.12 ng.L^{-1}, 0.6 ng.L^{-1}, 3 ng.L^{-1}, 15 ng.L^{-1}, 0.76 μg.L^{-1} and 3.8 μg.L^{-1} and doxorubicin, as positive control, at 0.86 μg.L^{-1}, 4.35 μg.L^{-1}, 0.02 mg.L^{-1}, 1.1 mg.L^{-1}, 5.43 mg.L^{-1}) in triplicate and incubated during 24, 48, and 72h at 28°C. Then, the medium was removed and 150 μL of the MTT solution (0.40 mg.L^{-1}) were added into each well and plates were incubated in a dry oven for 4 h at 28°C. After this, the medium containing MTT was removed, and the plates were dried at 37°C overnight. On the next day, 150 μL of DMSO (99.5%) was used to dilute the produced formazan. The plates containing the final volumes were analyzed by a microplate reader at 570 nm (Infinite 200, Tecan). Samples exposed to only DMSO (negative control) were considered as 100% cell viability, while blank wells (no cells added) were considered as 0% cell viability. The percentage of the viable cells was calculated using the following formula: (%) = [100 × (sample absorbance – blank absorbance)/(DMSO control absorbance - blank absorbance)].

To perform the TB exclusion test, ZFL cells were seeded at 4×10^4 cells.mL^{-1} 24 h prior to trabectedin treatment at concentrations 0.04, 0.08, and 0.15 μg.L^{-1}. After a 24 h exposure, cells were recovered by trypsinization, followed by centrifugation. Recovered cells were resuspended in 90 μL and stained with 0.4% TB (10 μL). Subsequently, viable and non-viable cells were counted using a Neubauer chamber. Results were expressed as a percentage of viable cells.

2.4. Flow cytometry

The ZFL cells morphology was evaluated by flow cytometry (Becton Dickinson FACScan) (Cui et al., 2015). ZFL cells were seeded at 4×10^4 cells.mL^{-1} 24 h prior to trabectedin treatment. After the exposure to trabectedin at concentrations of 0.04, 0.08 and 0.15 μg.L^{-1}, cells were suspended in 1 mL of Phosphate-buffered saline (PBS) 1x and immediately analyzed. The Fluorescence Activated Cell Sorting (FACS) parameters, Forward Scatter (FSC) and Side Scatter (SSC) and region settings were the same throughout all experiments. The data regarding 10,000 cells per replicate were analyzed using the software FlowJo ®60.

2.5. Immunofluorescence analysis

Cells were fixed with a 3.7% formaldehyde in 1x Phosphate Buffered Saline (PBSA - Ca^{2+} and Mg^{2+} free) (pH 7.4) and the plasma membrane was permeabilized with 0.5% Triton X-100 for 20 minutes. Then, cells were incubated overnight with a mix of primary monoclonal anti-α and anti-β tubulin antibodies into a moist chamber. After three times washing with PBSA, the cells were incubated for 1 hour with the fluorochrome-conjugated secondary antibody. Subsequently, the preparations with the F-actin were stained with Alexa 633-phalloidin for 60 minutes and the nuclei were stained with 4′,6-diamidino-2-phenylindole (1 μg.mL^{-1}) (DAPI). Finally, the cytological preparations were mounted on the microscopic slide with Vectashield (Vector) and observed under the Lionheart (Biotek, Vermont, USA) fluorescence microscope (Wang et al., 2019).

2.6. Fish embryo toxicity (FET) assay

Zebrafish eggs were collected within 1 hour after natural mating of 20 sexually mature and healthy couple fish. All FET tests were carried out following the OECD 236 guideline (OECD, 2013) and the methodology described by Lammer et al. (2009), with some adaptations. The newly fertilized eggs were checked under a stereomicroscope (Stereoscopic Zoom Microscope-SMZ 1500, Nikon) and eggs with cleavage irregularities, injuries, or other malformations including opaque eggs were discarded.

The test was conducted in 24-well plates with one embryo in 2 mL of solution per well. Embryo-larvae zebrafish (3 hours post fertilization - hpf) were exposed to trabectedin at increasing concentrations (6.25, 11.85, 22.49, 42.65, 80.90, and 153.44 μg.L^{-1}) with 20 embryos per condition, including two controls (negative and solvent DMSO) as well as a positive control (4 mg.L^{-1} 3,4-dichloroaniline (3.4-DCA)), as recommended by the OECD 236 guideline (OECD, 2013). A preliminary toxicity test was performed in order to establish the range of concentrations used in this test (data not shown). Zebrafish embryos and larvae were checked every 24h during a 96h exposure for mortality (*e.g.* coagulated embryos, lack of heartbeat in the larvae), hatching success and morphological malformations (such as lack of somite formation, presence of edema, lack of equilibrium, tail malformations, spinal curvature and pigmentation). A semi-renewal of the AA was performed in all experiments every 48 hours by replacing half of the exposure medium with a freshly prepared one.

2.7. Swimming behavior in larvae

Zebrafish larvae were subjected to behavioral tests after exposure to 6.25, 11.85, 22.49 and 42.65 μg.L^{-1} of trabectedin and the negative and solvent (DMSO) controls, at 120 hpf to ensure the swimming bladder inflation, thereby allowing the free larval swimming. The chosen concentrations correspond to trabectedin concentrations causing no malformations to *D. rerio* larvae derived from the FET assay. Exposures were conducted in 20 mL glass crystallizing dishes filled with respective test solution, containing 10 embryos each. Dead larvae or larvae that displayed physical abnormalities were excluded from this experiment. Initially, larvae were individually and, to avoid bias, randomly allocated to 96-well plates (n=12/concentration) and submitted to 15 minutes of an acclimatization period. Finally, the Zebrabox - ZEB 478 (Viewpoint Life Sciences, Lyon, France) was used for digital scans of the larvae locomotor activity for 20 minutes, alternating 5-minute light and dark periods to assess effects of the AA in response to a light stimulus or inhibition, as typically zebrafish larvae move more actively during dark periods (Burgess and Granato, 2007). A threshold of 15 (gray level) was applied for background correction. The parameters total distance, velocity and freezing behavior, calculated through the ratio between the total duration of inactive periods and the duration of the test, were measured.

2.8. Statistical analysis

Concentration-response curves were drawn using Prism 9.1.0 (GraphPad, four-parameter logistic curve) to determine LC_{50} and IC_{50} values from acute effects in *in vivo* and *in vitro* data and EC_{50} from the zebrafish embryo-larvae abnormalities effects data. The goodness of fit was analyzed by the coefficient of correlation (r^2).

Negative and solvent control (DMSO) were compared using Student t-tests. Significant differences (p-value < 0.05) between solvent control and exposed samples were inferred using one-way ANOVA. In cases of failure of parametric analysis prerequisites normality and homoscedasticity test, a Mann-Whitney U test and an ANOVA on ranks (Kruskal–Wallis) were performed. Significant differences were determined with Dunn's and Dunnett's post hoc test for nonparametric and parametric analysis, respectively. Test statistics and analysis of normality and homogeneity of variances were performed using the software IBM SPSS statistical software (version 25). Figures were designed with Prism 9.1.0 (GraphPad).

3. Results

3.1. Effects of trabectedin in ZFL cells viability and morphology

Trabectedin was strongly cytotoxic to ZFL cells after 24, 48 and 72 h, with IC_{50} values in the μg.L^{-1} range (Table 1). Doxorubicin, used as a reference compound, showed IC_{50} values 50, 40 and 12 times higher than the ones observed to trabectedin after 24, 48 and 72 h incubation, respectively (Table 1).

The TB analysis revealed that trabectedin at all tested concentrations (0.04, 0.08 and 0.15 μg.L^{-1}) caused a significant decrease in ZFL cell viability compared to solvent control (DMSO) ($p = 0.003$, $p < 0.001$, and $p < 0.001$, respectively, $F = 28.35$ and $df = 12$) (Figure 1A). As no significant statistical difference was observed between negative and solvent control in this study, the solvent control was chosen to compare our data. The FACS analysis was performed to examine cell size and internal complexity (*i.e.* granularity), defined by the FCS and SSC axis, respectively. The gate threshold that represents the morphological pattern of control cells includes a significant lower number of events for all trabectedin treatments (Figure 1B). Moreover, with the increase in trabectedin concentration, ZFL cells showed a reduction in the diameter and granularity (Figure 1B and 1C).

To further observe the morphology of ZFL cells, immunofluorescence staining of microtubules, F-actin and nucleus was carried out. As shown in the photomicrographs (Figure 2), trabectedin-treated cells seemed to assume a rounded shape and retracted nuclei, microfilaments and microtubules, whereas control ones presented a more elongated morphology. One of the most notable effects was the distribution of actin filaments, densely marked on the periphery of the control cells, but with diffuse orientation in cells exposed to trabectedin. Such alterations were highly evidenced in cells treated with the highest concentration of the drug (Figure 2).

Table 1
Cytotoxicity of trabectedin and doxorubicin (positive control) against ZFL cells as analyzed by the MTT assay. IC_{50} data are means (95% confidence intervals) and R^2 is the coefficient of correlation.

	24 h	48 h	72 h
Trabectedin			
IC_{50} (μg. L^{-1})	1.75 (1.24-2.48)	1.22 (0.55-2.21)	0.99 (0.82-1.62)
R^2	0.86	0.77	0.91
Doxorubicin			
IC_{50} (μg. L^{-1})	86.96 (30.43-227.19)	48.92 (20.65-108.16)	11.96 (7.61-17.39)
R^2	0.72	0.73	0.93

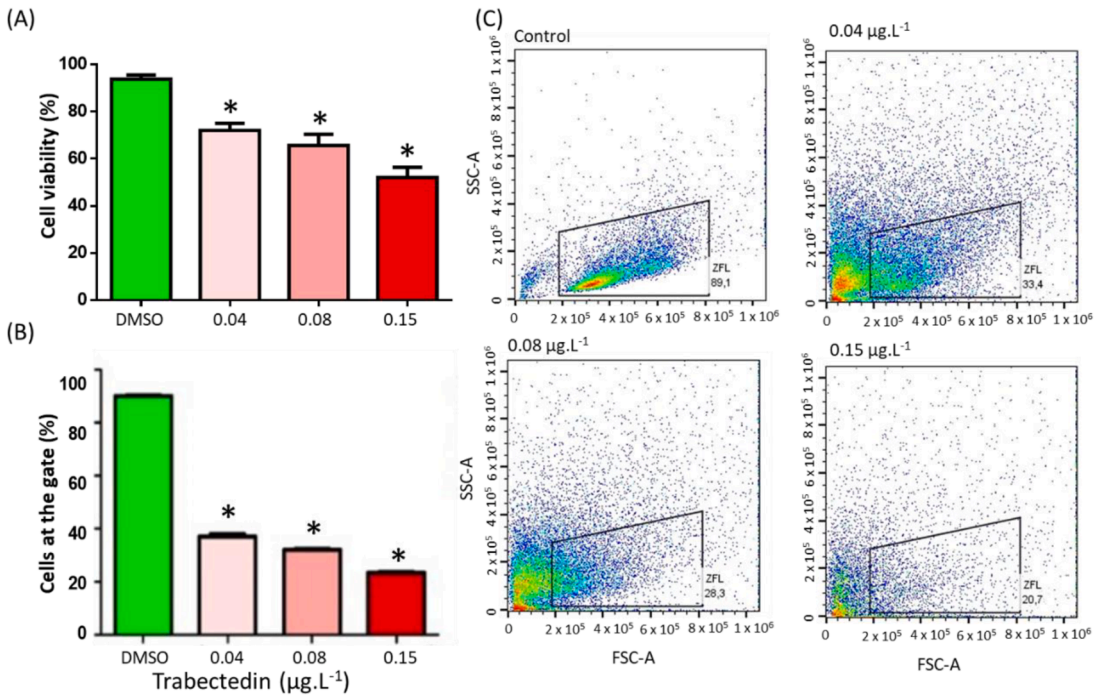

Fig. 1. Effect of trabectedin at 0.04, 0.08, and 0.15 µg.L^{-1} on ZFL cells viability measured by TB exclusion method **(A)** and by flow cytometry **(B and C).** The gate selected (Figure C) showed the viable cells population considering size (FSC) and granularity (SSC). Data are presented as mean values ± S.E.M from three independent experiments. * $p<0.05$, compared to solvent control (DMSO) by ANOVA followed by Dunnett's test.

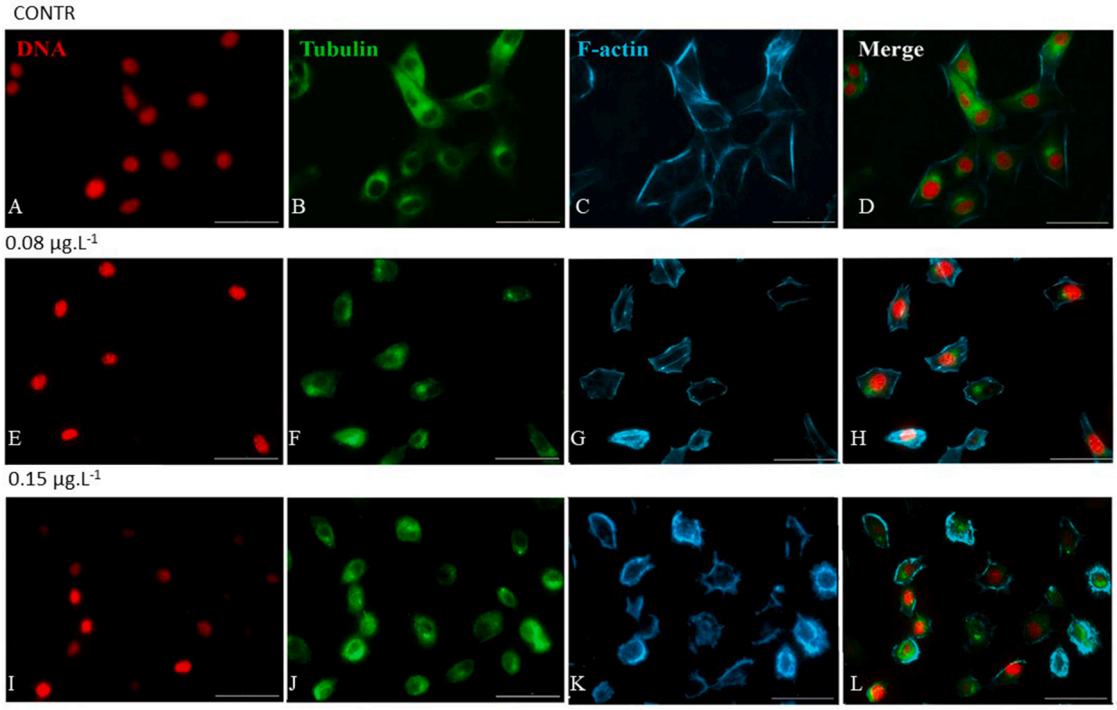

Fig. 2. Immunofluorescence staining of control (A-D) and trabectedin (E – H and I - K)-treated (0.08 and 0.15 µg.L^{-1}, respectively) ZFL cells after 24 h of exposure. The nuclei were stained with DAPI (red, A, E and I), the microtubules evidenced by monoclonal antibodies against α and β tubulin and anti-mouse FITC-antibody (green, B, F and J) and F-actin stained with Alexa 633-phalloidin (blue, C, G and K). Merged staining showed in panels D. H and L. The scale bar represents 30 µm.

3.2. Effects on embryo- larvae survival and development

The acute effect caused by trabectedin on zebrafish embryo-larvae is depicted in Table 2 and Figure 3. Trabectedin caused mortality at 24h of exposure, with a LC_{50} of 95.5 µg.L^{-1}. In the following days of exposure, mortality increased presenting a LC_{50} value of 77.55 µg.L^{-1} at 96h (Table 2).

Exposure to trabectedin also caused sublethal effects to the *D. rerio* embryo-larvae, such as developmental abnormalities including somite alterations, pericardial edema, tail malformations and lack of

Table 2
Effects of trabectedin in zebrafish embryo-larvae survival. LC_{50} data are means (95% confidence intervals) and R^2 is the coefficient of correlation.

	24 h	48 h	72 h	96 h
LC_{50} (μg.L^{-1})	95.61 (91.34- 100.03)	83.12 (-)	81.46 (-)	77.55 (-)
R^2	0.99	0.96	0.93	0.99

Note: - not defined.

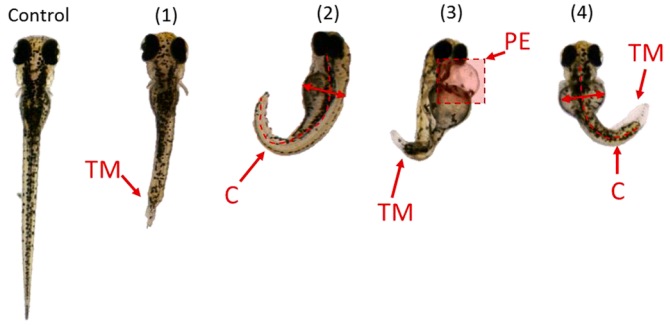

Fig. 3. Photomicrographs representative of the teratogenic abnormalities observed in *Danio rerio* larvae at 96 hpf of exposure to trabectedin (1-4). (1 and 2): Larvae exposed to trabectedin at 42.66 μg.L^{-1}, and (3 and 4): Larvae exposed to trabectedin at 80.75 μg.L^{-1}. Arrows indicate developmental abnormalities: spinal curvature (C), tail malformations (TM) and pericardial edema (PE).

equilibrium (Figure 3). At 24 hpf, the only observable effect was somite alterations, presenting an EC_{50} of 75.42 μg.L^{-1}. In turn, pericardial edemas were observed in the following exposure days, presenting an EC_{50} of 66.28, 74.66, and 75.42 μg.L^{-1} at 24, 48 and 96 hpf, respectively (Table 3). Increasing values do not mean that zebrafish have recovered but rather that those with edemas died in the subsequent days, thus resulting in an apparent decrease of the sublethal effect measured. Tail malformations were also observed, with an intensification of this effect at 72 hpf with an EC_{50} of 42.66 μg.L^{-1} (Table 3). The lack of larvae equilibrium was perceived at 96 hpf (Table 3).

Regarding mortality and malformations at 96 h, the LOEC value, expressed by the lowest concentrations at which an effect was seen, was rendered by 42.66 μg.L^{-1}, while the NOEC value, defined as the highest concentration at which no effect was seen, was met at 22.47 μg.L^{-1}.

3.3. Effects of trabectedin on behavior

A significant increase of velocity and total distance covered by larvae exposed to the highest concentration of trabectedin was observed during the first dark period (Figure 4). No further behavioral differences were observed during the remaining concentrations and stages. Thus, the LOEC value corresponded to zebrafish locomotor behavior was rendered by 42.66 μg.L^{-1}, while the NOEC was met at 22.47 μg.L^{-1}, similar to those for survival and malformations.

Table 3
Effects of trabectedin on developmental parameters of zebrafish embryo-larvae. EC_{50} (μg.L^{-1}) data are means (95% confidence intervals).

Developmental parameters	24 h	48 h	72 h	96 h
Somite alteration	75.26 (-)	n.c.	n.c.	n.c.
Tail malformations	n.c.	80.45 (-)	42.77 (38.33 - 47.71)	46.78 (40.68 - 52.19)
Lack of equilibrium	n.c.	n.c.	n.c.	52.59 (46.92 - 58.95)
Pericardial edema	n.c.	66.45 (82.89 - 91.78)	75.53 (-)	76.79 (-)

Note: n.c. not calculated because the observed effects were below 50% level; - not determined.

4. Discussion

The main purpose of this study was to evaluate the ecotoxicity of the anticancer agent trabectedin by establishing an approach of *in vitro* and *in vivo* experiments with different endpoints using zebrafish as a model. Considering the lack of information on trabectedin ecotoxicity, and the potential occurrence in the environment, the present study is highly innovative for being the first ecotoxicological report regarding trabectedin.

ZFL cells were as sensitive to trabectedin as tumor cells with IC_{50} values in the μg.L^{-1} range. Trabectedin (NSC 648766) presented a mean GI_{50} of 1.48μg.L^{-1} considering the NCI-60 cell line panel, (www.dtp.cancer.gov, accessed 26 September 2020). Using human cancer cells from different histological origins, it was shown that trabectedin cellular effects involves a multitude of mechanisms, most of which are related to impaired transcription and DNA damage (Di Giandomenico et al., 2013). In this sense, the adducts formed by trabectedin and DNA resemble an inter-strand cross-linking lesion that avoids binding of transcription factors to DNA and interrupts the transcription process itself, thus impacting various downstream signaling (Bueren-Calabuig et al., 2011). Additionally, trabectedin inhibits active transcription elongation, which is mediated by RNA polymerase II in different human cancer cells, including Edwing's sarcoma, renal cancer cells and transformed fibroblasts at 7.62 μg.L^{-1} (equivalent to the reported 10 nM) (Aune et al., 2008; Larsen et al., 2016). Herein, the cytotoxic observed effects are compatible with those described for cancer cells, although it was not evaluated at a molecular level to establish any involvement of transcription factors modulation in ZFL cells.

It has been reported that trabectedin acts on a high diversity of tumor cell lines. Hoda et al. (2016) observed that trabectedin caused a massive reduction of viable malignant pleural mesothelioma cells and frequent chromatin condensation, indicative of apoptotic cell death induction after 24-hour exposure at 1.90 μg.L^{-1} (equivalent to the reported 2.5 nM). Under the same conditions, trabectedin was also toxic to multiple myeloma plasma cells and adrenocortical carcinoma cells, it was able to cause DNA damage, reactive oxygen species (ROS) production and cell cycle arresting (Abate et al., 2020; Cucè et al., 2019).

The morphological changes caused by trabectedin in ZFL cells are consistent with the results in human cancer cells. Preusser et al. (2012) observed the potent disruption of the microfilament system combined with the round-up of human meningioma cells caused by trabectedin at 19.04 μg.L^{-1} (equivalent to the reported 25 nM). Furthermore, trabectedin in combination with taurolidine caused severe morphological alterations in human fibrosarcoma cells, including the disintegration of the subconfluent cell groups and cell shrinkage (Harati et al., 2012). These results open up the possibility to further study trabectedin toxicity in these cells, since hepatotoxicity is the most studied adverse effect caused by trabectedin in cancer patients (Laurenty et al., 2013).

Turning to a more complex system, trabectedin was further evaluated in the zebrafish embryo-larval development, showing, as expected, significant lethal effects at concentrations 40-100 times higher than those toxic to ZFL cells. Comparing the LC_{50} values of trabectedin presented herein with other anticancer compounds, trabectedin was highly toxic to the zebrafish embryo-larvae. Kovács et al. (2016) tested four cytostatic drugs (5-fluorouracil, cisplatin, etoposide, and imatinib mesylate) to zebrafish larvae and the most lethal of them, imatinib mesylate, was 3 log units less potent than trabectedin. The 96 h LC_{50} of the AAs taxol and triptolide were about 1 log unit higher compared to trabectedin results obtained from our study (Gao et al., 2014). The most common trabectedin event related to mortality in cancer patients is rhabdomyolysis, defined as the escape of intracellular muscular components, like electrolytes and myoglobin, leading to a condition of muscle dissolution (Hohenegger, 2012; Pick and Nystrom, 2010;

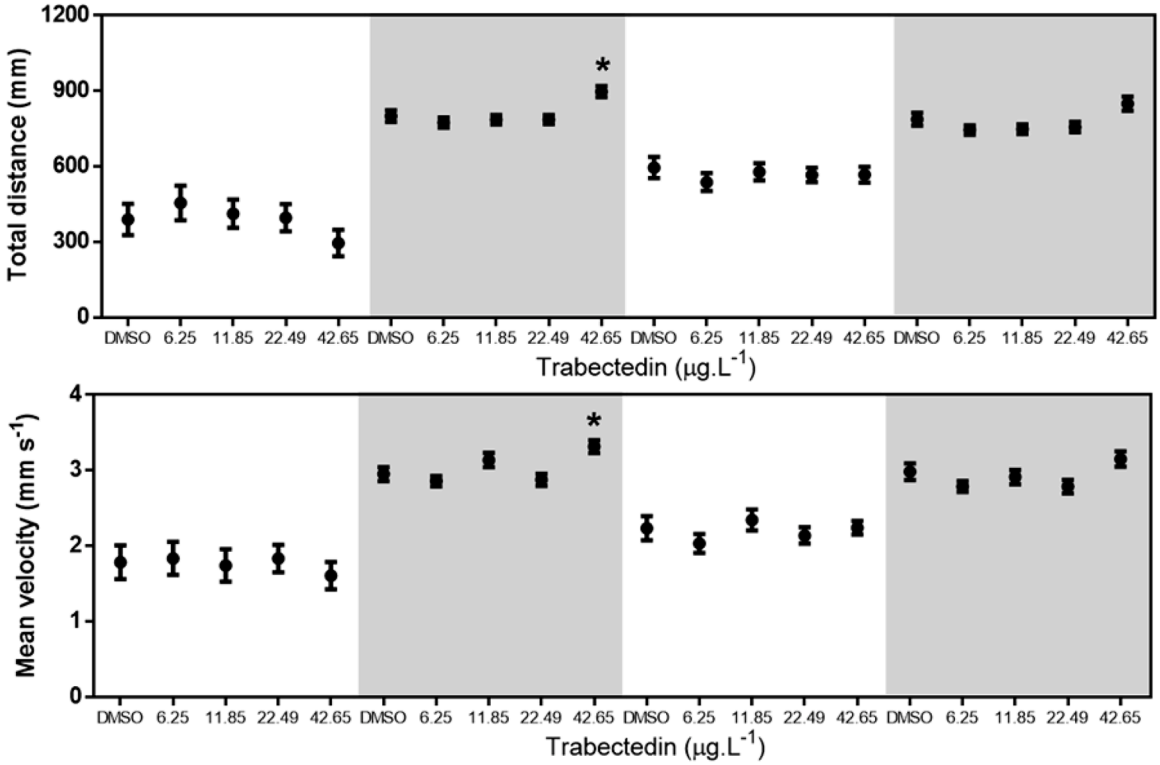

Fig. 4. Total distance covered **(A)** and mean velocity **(B)** by zebrafish larvae (120 hpf) after exposure to trabectedin, during light (white area) and dark (grey area) periods. Results are presented as mean value ± standard error of the mean. Asterisks (*) indicate statistically significant differences ($p<0.05$) of trabectedin treatments compared to DMSO.

Stoyianni et al., 2011). Eggs exposed to trabectedin presented an aspect of muscle disintegration or somite alterations at 24 hpf that triggered the organism's death on the next days of exposure.

Trabectedin is considered a teratogenic drug to humans (Fala, 2016). In this study, distinct malformations were observed in the zebrafish embryos and larvae at 96 hpf, with the most prominent effect being tail malformations (shortening of the tail and spinal curvature). The cellular process for tail development may be affected by trabectedin through its main mechanism of action. As previously mentioned, trabectedin inhibits DNA transcription, as such misexpression of transcription factors involved to the disruption of the zebrafish's tail embryonic development was observed due to xenobiotics exposure (Qian et al., 2020; Rhyu et al., 2019).

Trabectedin clinical trials did not detect significant cardiac risk to humans (Lebedinsky et al., 2011). Nevertheless, in our study, pericardial edema was observed from 48 h of trabectedin exposure and, after this period, it preceded to total larval mortality, therefore, suggesting trabectedin to promote cardiotoxicity. Incardona et al. (2004) detected that one of the possible causes of pericardial edema in zebrafish larvae is the insufficient synthesis of troponin T, an essential component of the sarcomere in cardiomyocytes and a cardiotoxicity predictor (Katsurada et al., 2014). Lurbinectedin, an alkaloid that derives from trabectedin and has mechanisms of action similar to this AA, caused a reduction of troponin T in mice (Bearing et al., 2020), suggesting that trabectedin can promote the same cardiotoxicity effect.

In this study, zebrafish larvae exposed to trabectedin were observed having lack of equilibrium (after stimulation failed to return to their normal position, thus remaining with the ventral abdomen oriented towards the surface). This effect may be caused by the morphological abnormalities in the tail provoked by trabectedin. Although, damage to hair cells caused by AAs can be found in the lateral line and inner ears of fish and possibly affect negatively their balance coordination (Kovács et al., 2016).

The effects of trabectedin on larvae swimming behavior was analyzed, and increased velocity and increased total distance moved by larvae under dark condition were observed at concentration of 42.66 µg. L^{-1}. Behavior analysis of different AAs using the zebrafish larvae found reversed results from the ones in this study. Ng et al. (2020) observed that 5-FU decreased the distance traveled and mean velocity as well as reduced time moving to zebrafish larvae after 4 and 6 days of exposure, respectively. Additionally, Kim et al. (2014) reported that cisplatin caused a reduction in total swimming distance, peak and mean swimming velocity of zebrafish larvae, attributing this effect to an ototoxicity induction. The increase or decrease in locomotion activity observed in these studies could be associated with effects on different targets; for example, anxiogenic compounds may induce hyperactivity in larvae during dark periods (Steele et al., 2018). In this study, activity decreased briefly during transitions from dark to light. The ecological consequences of exposure to drugs that modulate the zebrafish's nervous system and cause locomotor impairment are involved in the capability of prey capture and increase vulnerability to predation (Weis et al., 2000).

To date, no *in vitro* trabectedin studies using non-cancer cells have been found confirming the innovative and pioneering characteristics of our study. The fact that we observed that the sensitivity of ZFL cells to trabectedin being similar to target cells at several endpoints is an important warning about the potential environmental damage of AAs present in the aquatic environment. Additionally, the use of the *in vivo* model provided information of the possible effects at a higher organismal level. This work highlights the valuable combination of *in vitro* and *in vivo* models in order to better perceive the possible toxic effects of an AA from an environmental protection perspective. Moreover, the results obtained indicate the ZFL cells as a satisfactory model as an alternative to animal testing in hazard assessments. Such approaches provide robustness and reliability for a more thorough hazard and, eventually, risk assessment.

5. Conclusions

The present study revealed the anticancer agent trabectedin to affect zebrafish in relevant *in vitro* and *in vivo* ecotoxicological setups, altering from cytoskeleton components of the ZFL cell line, to the development of embryo-larvae and locomotion of larvae zebrafish. Trabectedin is a highly toxic drug, and affects zebrafish cells (non-target and normal cells) at the same level as tumor cells. These findings support the need of studies like this one to infer on the potential environmental hazards of trabectedin, considering the wide use of this pharmaceutical. The difference in sensitivity of zebrafish cells and embryos highlight the potential use of zebrafish cells to decrease uncertainties and promote protection of freshwater systems. The zebrafish larvae-embryo-cell line system revealed to be a suitable tool for assessing the toxicity of anticancer compounds in a relevant ecological setting. Some concerns need to be tackled regarding the chemical determination and monitorization of trabectedin in freshwater ecosystems.

CRediT authorship contribution statement

Évila Pinheiro Damasceno: Conceptualization, Formal analysis, Investigation, Writing – original draft, Visualization. **Ives Charlie-Silva:** Conceptualization, Formal analysis, Investigation, Writing – original draft, Visualization. **Glaucia Maria Machado-Santelli:** Resources, Writing – review & editing, Visualization, Supervision. **Anali M.B. Garnique:** Investigation, Visualization. **João Agostinho Machado-Neto:** Writing – review & editing, Supervision. **Simone Aparecida Teixeira:** Investigation, Writing – review & editing. **Paula C. Jimenez:** Formal analysis, Investigation, Writing – review & editing, Visualization, Supervision. **Diana Carneiro:** Investigation. **Amadeu M.V.M. Soares:** Resources, Supervision, Funding acquisition. **Leticia V. Costa-Lotufo:** Conceptualization, Resources, Writing – review & editing, Supervision, Project administration, Funding acquisition. **Susana Loureiro:** Conceptualization, Resources, Writing – review & editing, Supervision, Project administration. **Maria D. Pavlaki:** Conceptualization, Investigation, Resources, Writing – review & editing, Supervision, Project administration, Funding acquisition.

Declaration of Competing Interests

The authors declare that they have no known competing financial interests or personal relationships that could have appeared to influence the work reported in this paper.

Acknowledgements

This study was supported by a Ph.D. grant (PD/BD137978/2018) attributed to Évila Damasceno through the BEGC- Biology and Ecology of Global Changes Ph.D. program financed by the Portuguese Science and Technology Foundation-FCT (Fundação para a Ciência e Tecnologia). Ives Charlie-Silva has a post-doctoral fellowship from São Paulo Research Foundation-FAPESP (#2019/19939-1). This work was supported by the bilateral project EMPHASIS (PTDC/CTA-AMB/31180/2017) funded by FEDER, through COMPETE2020 - Programa Operacional Competitividade e Internacionalização (POCI), and by national funds (OE), through FCT/MCTES and (#2018/07098-0 and #2015/17177-6) through FAPESP. Thanks are due to FCT/MCTES for the financial support to CESAM (UIDP/50017/2020+UIDB/50017/2020+LA/P/0094/2020), through national funds. The authors would also like to thank Ana Rita Almeida, Abel Ferreira and Sandra Gonçalves for the technical support provided during this work.

Supplementary materials

Supplementary material associated with this article can be found, in the online version, at doi:10.1016/j.envadv.2022.100208.

References

Abate, A., Rossini, E., Bonini, S.A., Fragni, M., Cosentini, D., Albero, G., Tiberio, M., Benetti, D., Hantel, C., Lagan, M., Grisanti, S., Terzolo, M., Memo, M., Berruti, A., Sigala, S., 2020. Cytotoxic Effect of Trabectedin In Human Adrenocortical Carcinoma Cell Lines and Primary Cells. Cancers 12, 1–15. https://doi.org/10.3390/cancers12040928.

Almeida, A.R., Jesus, F., Henriques, J.F., Andrade, T.S., Barreto, Â., Koba, O., Giang, P.T., Soares, A.M.V.M., Oliveira, M., Domingues, I., 2019. The role of humic acids on gemfibrozil toxicity to zebrafish embryos. Chemosphere 220, 556–564. https://doi.org/10.1016/j.chemosphere.2018.12.133.

Aune, G.J., Takagi, K., Sordet, O., Antony, S., Bohr, V.A., Pommier, Y., 2008. Cancer therapy : preclinical von Hippel-Lindau ^ coupled and T ranscription-coupled nucleotide excision repair ^ dependent degradation of RNA polymerase II in response toT rabectedin. Cancer Ther. Preclin. 14, 6449–6456. https://doi.org/10.1158/1078-0432.CCR-08-0730.

Bearing, M., Colon, C., Aquila, G., David, A., Cecconi, R., Forti, M., Frapolli, R., Bello, E., Novelli, D., Russo, I., Licandro, S.A., Staszewsky, L., Martinelli, G.B., Talamini, L., Pasetto, L., Resovi, A., Scanziani, E., Careccia, G., Emilie, V., 2020. Without affecting tumor growth or cachexia 1–25.

Bueren-Calabuig, J.A., Giraudon, C., Galmarini, C.M., Egly, J.M., Gago, F., 2011. Temperature-induced melting of double-stranded DNA in the absence and presence of covalently bonded antitumour drugs: Insight from molecular dynamics simulations. Nucleic Acids Res 39, 8248–8257. https://doi.org/10.1093/nar/gkr512.

Burgess, H.A., Granato, M., 2007. Modulation of locomotor activity in larval zebrafish during light adaptation. J. Exp. Biol. 210, 2526–2539. https://doi.org/10.1242/jeb.003939.

Cucè, M., Gallo Cantafio, M.E., Siciliano, M.A., Riillo, C., Caracciolo, D., Scionti, F., Staropoli, N., Zuccalà, V., Maltese, L., Di Vito, A., Grillone, K., Barbieri, V., Arbitrio, M., Di Martino, M.T., Rossi, M., Amodio, N., Tagliaferri, P., Tassone, P., Botta, C., 2019. Trabectedin triggers direct and NK-mediated cytotoxicity in multiple myeloma. J. Hematol. Oncol. 12, 1–17. https://doi.org/10.1186/s13045-019-0714-9.

Cui, Y., Liu, W., Xie, W., Yu, W., Wang, C., Chen, H., 2015. Investigation of the effects of perfluorooctanoic acid (PFOA) and perfluorooctane sulfonate (PFOS) on apoptosis and cell cycle in a Zebrafish (Danio rerio) liver cell line. Int. J. Environ. Res. Public Health 12, 15673–15682. https://doi.org/10.3390/ijerph121215012.

D'Incalci, M., Badri, N., Galmarini, C.M., Allavena, P., 2014. Trabectedin, a drug acting on both cancer cells and the tumour microenvironment. Br. J. Cancer 111, 646–650. https://doi.org/10.1038/bjc.2014.149.

D'Incalci, M., Galmarini, C.M., 2010. A review of trabectedin (ET-743): a unique mechanism of action. Mol. Cancer Ther. 9, 2157–2163. https://doi.org/10.1158/1535-7163.MCT-10-0263.

Di Giandomenico, S., Frapolli, R., Bello, E., Uboldi, S., Licandro, S.A., Marchini, S., Beltrame, L., Brich, S., Mauro, V., Tamborini, E., Pilotti, S., Casali, P.G., Grosso, F., Sanfilippo, R., Gronchi, A., Mantovani, R., Gatta, R., Galmarini, C.M., Sousa-Faro, J. M.F., D'incalci, M., 2013. Mode of action of trabectedin in myxoid liposarcomas. Oncogene 33, 5201–5210. https://doi.org/10.1038/onc.2013.462.

Didkowska, J., Wojciechowska, U., Mańczuk, M., Lobaszewski, J., 2016. Lung cancer epidemiology: contemporary and future challenges worldwide. Ann. Transl. Med. 4, 1–11. https://doi.org/10.21037/atm.2016.03.11.

EMA, 2015. Yondelis (Trabectedin). PharmaDeals Rev.

Fala, L., 2016. Seventh annual payers' guide. Yondelis (Trabectedin) Approved for the Treatment of Unresectable or Metastatic Soft-Tissue Sarcomas. Payers' Guide.

Ferlay, J., Colombet, M., Soerjomataram, I., Mathers, C., Parkin, D.M., Piñeros, M., Znaor, A., Bray, F., 2019. Estimating the global cancer incidence and mortality in 2018: GLOBOCAN sources and methods. Int. J. Cancer 144, 1941–1953. https://doi.org/10.1002/ijc.31937.

Gajski, G., Gerić, M., Domijan, A.M., Garaj-Vrhovac, V., 2016. Combined cyto/genotoxic activity of a selected antineoplastic drug mixture in human circulating blood cells. Chemosphere 165, 529–538. https://doi.org/10.1016/j.chemosphere.2016.09.058.

Gao, X.P., Feng, F., Zhang, X.Q., Liu, X.X., Wang, Y.Bin, She, J.X., He, Z.H., He, M.F., 2014. Toxicity assessment of 7 anticancer compounds in zebrafish. Int. J. Toxicol. 33, 98–105. https://doi.org/10.1177/1091581814523142.

Ghosh, C., Zhou, Y.L., Collodi, P., 1994. Derivation and characterization of a zebrafish liver cell line. Cell Biol. Toxicol. 10, 167–176. https://doi.org/10.1007/BF00757560.

Gordon, E.M., Sankhala, K.K., Chawla, N., Chawla, S.P., 2016. Trabectedin for soft tissue sarcoma: current status and future perspectives. Adv. Ther. 33, 1055–1071. https://doi.org/10.1007/s12325-016-0344-3.

Harati, K., Chromik, A.M., Bulut, D., Goertz, O., Hahn, S., Hirsch, T., Klein-Hitpass, L., Lehnhardt, M., Uhl, W., Daigeler, A., 2012. TRAIL and taurolidine enhance the anticancer activity of doxorubicin, trabectedin and mafosfamide in HT1080 human fibrosarcoma cells. Anticancer Res 32, 2967–2984.

Higuchi, T., Miyake, K., Oshiro, H., Sugisawa, N., Yamamoto, N., Hayashi, K., Kimura, H., Miwa, S., Igarashi, K., Chawla, S.P., Bouvet, M., Singh, S.R., Tsuchiya, H., Hoffman, R.M., 2019. Trabectedin and irinotecan combination regresses a cisplatinum-resistant osteosarcoma in a patient-derived orthotopic xenograft nude-mouse model. Biochem. Biophys. Res. Commun. 513, 326–331. https://doi.org/10.1016/j.bbrc.2019.03.191.

Hoda, M.A., Pirker, C., Dong, Y., Schelch, K., Heffeter, P., Kryeziu, K., Van Schoonhoven, S., Klikovits, T., Laszlo, V., Rozsas, A., Ozsvar, J., Klepetko, W., Döme, B., Grusch, M., Hegedüs, B., Berger, W., 2016. Trabectedin is active against malignant pleural mesothelioma cell and xenograft models and synergizes with

chemotherapy and Bcl-2 inhibition in vitro. Mol. Cancer Ther. 15, 2357–2369. https://doi.org/10.1158/1535-7163.MCT-15-0846.
Hohenegger, M., 2012. Drug induced rhabdomyolysis. Curr. Opin. Pharmacol. 12, 335–339. https://doi.org/10.1016/j.coph.2012.04.002.
Incardona, J.P., Collier, T.K., Scholz, N.L., 2004. Defects in cardiac function precede morphological abnormalities in fish embryos exposed to polycyclic aromatic hydrocarbons. Toxicol. Appl. Pharmacol. 196, 191–205. https://doi.org/10.1016/j.taap.2003.11.026.
Jimenez, P.C., Wilke, D.V., Branco, P.C., Bauermeister, A., Rezende-Teixeira, P., Gaudêncio, S.P., Costa-Lotufo, L.V., 2020. Enriching cancer pharmacology with drugs of marine origin. Br. J. Pharmacol. 177, 3–27. https://doi.org/10.1111/bph.14876.
Katsurada, K., Ichida, M., Sakuragi, M., Takehara, M., Hozumi, Y., Kario, K., 2014. High-sensitivity troponin T as a marker to predict cardiotoxicity in breast cancer patients with adjuvant trastuzumab therapy. Springerplus 3, 1–7. https://doi.org/10.1186/2193-1801-3-620.
Kim, M.J., Choi, J., Kim, N., Han, G.C., 2014. Behavioral changes of zebrafish according to cisplatin-induced toxicity of the balance system. Hum. Exp. Toxicol. 33, 1167–1175. https://doi.org/10.1177/0960327114521046.
Kosjek, T., Heath, E., 2011. Occurrence, fate and determination of cytostatic pharmaceuticals in the environment. TrAC - Trends Anal. Chem. 30, 1065–1087. https://doi.org/10.1016/j.trac.2011.04.007.
Kovács, R., Bakos, K., Urbányi, B., Kövesi, J., Gazsi, G., Csepeli, A., Appl, Á.J., Bencsik, D., Csenki, Z., Horváth, Á., 2016. Acute and sub-chronic toxicity of four cytostatic drugs in zebrafish. Environ. Sci. Pollut. Res. 23, 14718–14729. https://doi.org/10.1007/s11356-015-5036-z.
Kümmerer, K., Haiß, A., Schuster, A., Hein, A., Ebert, I., 2016. Antineoplastic compounds in the environment—substances of special concern. Environ. Sci. Pollut. Res. 23, 14791–14804. https://doi.org/10.1007/s11356-014-3902-8.
Lachner, D., Oliveira, L.F., Martinez, C.B.R., 2015. Toxicology in vitro effects of the water soluble fraction of gasoline on ZFL cell line : cytotoxicity, genotoxicity and oxidative stress. TIV 30, 225–230. https://doi.org/10.1016/j.tiv.2015.11.008.
Lammer, E., Carr, G.J., Wendler, K., Rawlings, J.M., Belanger, S.E., Braunbeck, T., 2009. Is the fish embryo toxicity test (FET) with the zebrafish (Danio rerio) a potential alternative for the fish acute toxicity test? Comp. Biochem. Physiol. - C Toxicol. Pharmacol. 149, 196–209. https://doi.org/10.1016/j.cbpc.2008.11.006.
Larsen, A.K., Galmarini, C.M., D'Incalci, M., 2016. Unique features of trabectedin mechanism of action. Cancer Chemother. Pharmacol. 77, 663–671. https://doi.org/10.1007/s00280-015-2918-1.
Laurenty, A.P., Thomas, F., Chatelut, E., Bétrian, S., Le Guellec, C., Hennebelle, I., Le Guellec, S., Chevreau, C., 2013. Irreversible hepatotoxicity after administration of trabectedin to a pleiomorphic sarcoma patient with a rare ABCC2 polymorphism: a case report. Pharmacogenomics 14, 1389–1396. https://doi.org/10.2217/pgs.13.124.
Lebedinsky, C., Gómez, J., Park, Y.C., Nieto, A., Soto-Matos, A., Parekh, T., Alfaro, V., Roy, E., Lardelli, P., Kahatt, C., 2011. Trabectedin has a low cardiac risk profile: a comprehensive cardiac safety analysis. Cancer Chemother. Pharmacol. 68, 1223–1231. https://doi.org/10.1007/s00280-011-1614-z.
Li, D., Sun, W., Chen, H., Lei, H., Li, X., Liu, H., Huang, G.yong, Shi, W.jun, Ying, G.G., Luo, Y., Xie, L., 2022. Cyclophosphamide affects eye development and locomotion in zebrafish (Danio rerio). Sci. Total Environ. 805, 150460 https://doi.org/10.1016/j.scitotenv.2021.150460.
Manda, K., Präkelt, T., Schröder, T., Kriesen, S., Hildebrandt, G., 2020. Radiosensitizing effects of trabectedin on human A549 lung cancer cells and HT-29 colon cancer cells. Invest. New Drugs 38, 967–976. https://doi.org/10.1007/s10637-019-00852-x.
Ng, M., DeCicco-Skinner, K., Connaughton, V.P., 2020. Using zebrafish to assess the effect of chronic, early developmental exposure to environmentally relevant concentrations of 5-fluorouracil and leucovorin. Environ. Toxicol. Pharmacol. 76 https://doi.org/10.1016/j.etap.2020.103356.
OECD, 2013. OECD guidelines for the testing of chemicals : OECD guidelines for the testing of chemicals June 2000 1–44.
Parrella, A., Kundi, M., Lavorgna, M., Criscuolo, E., Russo, C., Isidori, M., 2014a. Toxicity of exposure to binary mixtures of four anti-neoplastic drugs in Daphnia magna and Ceriodaphnia dubia. Aquat. Toxicol. 157, 41–46. https://doi.org/10.1016/j.aquatox.2014.09.012.
Parrella, A., Lavorgna, M., Criscuolo, E., Russo, C., Fiumano, V., Isidori, M., 2014b. Acute and chronic toxicity of six anticancer drugs on rotifers and crustaceans. Chemosphere 115, 59–66. https://doi.org/10.1016/j.chemosphere.2014.01.013.
Pick, A.M., Nystrom, K.K., 2010. Fatal hepatic and renal toxicity as a complication of trabectedin therapy for radiation-induced sarcoma. J. Oncol. Pharm. Pract. 16, 269–272. https://doi.org/10.1177/1078155209352821.
Preusser, M., Spiegl-Kreinecker, S., Lötsch, D., Wöhrer, A., Schmook, M., Dieckmann, K., Saringer, W., Marosi, C., Berger, W., 2012. Trabectedin has promising antineoplastic activity in high-grade meningioma. Cancer 118, 5038–5049. https://doi.org/10.1002/cncr.27460.
Qian, L., Liu, J., Lin, Z., Chen, X., Yuan, L., Shen, G., Yang, W., Wang, D., Huang, Y., Pang, S., Mu, X., Wang, C., Li, Y., 2020. Evaluation of the spinal effects of phthalates in a zebrafish embryo assay. Chemosphere 249, 126144. https://doi.org/10.1016/j.chemosphere.2020.126144.
Rhyu, D.Y., Lee, H., Tanguay, R.L., Kim, K.T., 2019. Tris(1,3-dichloro-2-propyl) phosphate (TDCIPP) disrupts zebrafish tail fin development. Ecotoxicol. Environ. Saf. 182, 109449 https://doi.org/10.1016/j.ecoenv.2019.109449.
Santana-Viera, S., Montesdeoca-Esponda, S., Sosa-Ferrera, Z., Santana-Rodríguez, J.J., 2016. Cytostatic drugs in environmental samples: An update on the extraction and determination procedures. TrAC - Trends Anal. Chem. 80, 373–386. https://doi.org/10.1016/j.trac.2015.08.016.
Santos, M.S.F., Franquet-Griell, H., Lacorte, S., Madeira, L.M., Alves, A., 2017. Anticancer drugs in Portuguese surface waters – Estimation of concentrations and identification of potentially priority drugs. Chemosphere 184, 1250–1260. https://doi.org/10.1016/j.chemosphere.2017.06.102.
Steele, W.B., Kristofco, L.A., Corrales, J., Saari, G.N., Haddad, S.P., Gallagher, E.P., Kavanagh, T.J., Kostal, J., Zimmerman, J.B., Voutchkova-Kostal, A., Anastas, P., Brooks, B.W., 2018. Comparative behavioral toxicology with two common larval fish models: exploring relationships among modes of action and locomotor responses. Sci. Total Environ. 640–641, 1587–1600. https://doi.org/10.1016/j.scitotenv.2018.05.402.
Stoyianni, A., Kapodistrias, N., Kampletsas, E., Pentheroudakis, G., Pavlidis, N., 2011. Trabectedin-related rhabdomyolysis: an uncommon but fatal toxicity. Tumori J. 97, 252–255. https://doi.org/10.1177/030089161109700223.
Wang, J., Han, S.L., Lu, D.L., Li, L.Y., Limbu, S.M., Li, D.L., Zhang, M.L., Du, Z.Y., 2019. Inhibited lipophagy suppresses lipid metabolism in zebrafish liver cells. Front. Physiol. 10, 1–9. https://doi.org/10.3389/fphys.2019.01077.
Weis, J.S., Smith, G., Santiago-Bass, C., 2000. Predator/prey interactions: A link between the individual level and both higher and lower level effects of toxicants in aquatic ecosystems. J. Aquat. Ecosyst. Stress Recover. 7, 145–153. https://doi.org/10.1023/A:1009923414208.
Załeska-Radziwiłł, M., Affek, K., Rybak, J., 2014. Ecotoxicity of chosen pharmaceuticals in relation to micro-organisms-risk assessment. Desalin. Water Treat. 52, 3908–3917. https://doi.org/10.1080/19443994.2014.887503.
Zhu, G., Zhao, M., Han, Q., Tan, Y., Sun, Y., Bouvet, M., Singh, S.R., Ye, J., Hoffman, R. M., 2019. Combination of trabectedin with oxaliplatinum and 5-fluorouracil arrests a primary colorectal cancer in a patient-derived orthotopic xenograft mouse model. Anticancer Res. 39, 5999–6005. https://doi.org/10.21873/anticanres.13805.